Thermal-fluid coupling analysis of oil shale pyrolysis and displacement by heat-carrying supercritical carbon dioxide

Author(s): Shuai, Zhao; Lü, Xiaoshu; Li, Qiang; Sun, Youhong

Title: Thermal-fluid coupling analysis of oil shale pyrolysis and displacement by heat-carrying supercritical carbon dioxide

Year: 2020

Version: Final draft

Please cite the original version:

Shuai, Z., Lü, X., Li, Q. & Sun, Y. (2020). Thermal-fluid coupling analysis of oil shale pyrolysis and displacement by heat-carrying supercritical carbon dioxide. *Chemical Engineering Journal* 394. https://doi.org/10.1016/j.cej.2020.125037

Thermal-fluid coupling analysis of oil shale pyrolysis and displacement byheat-carrying supercritical carbon dioxide

Zhao Shuai[a,b], Lü Xiaoshu[b,c,d], Li Qiang[b], Sun Youhong[b,*]

[a] *School of Mines, China University of Mining and Technology, Xuzhou 221116, China*
[b] *Construction Engineering College of JiLin University, Changchun 130000, China*
[c] *Department of Electrical Engineering and Energy Technology, University of Vaasa, P.O. Box 700, FIN-65101, Finland*
[d] *Department of Civil Engineering, Aalto University, P.O.Box. 11000, FIN-02130, Finland*

HIGHLIGHTS

- Considering the coupling of displacement and extraction in the process of oil shale pyrolysis.
- Supercritical carbon dioxide was as a heat transfer carrier to pyrolysis oil shale.
- The entrance effect on heat and mass transfer was considered.
- High pressure promotes the secondary cracking of oil and gas, which is beneficial to the increase of short chain alkanes

ABSTRACT

Supercritical carbon dioxide (SC-CO₂) has advantages in solubility and diffusion. It is suitable for extracting organic matter in porous media as heat-carrying fluid. This paper investigates whether supercritical carbon dioxide can promote the pyrolysis of oil shale using both laboratory experiments and numerical simulations. The diffusion and velocity distribution of heat carrying supercritical carbon dioxide in oil shale are simulated by using COMSOL Multiphysics. The results show that at the pressure 7.8 mpa, while the injection temperature is 400 °C and the injection flow rate is 2.5–9 ml/s, both the axial displacement rate and the front pyrolysis rate increase with increasing injection flow rate and pyrolysis time. The pyrolysis front gradually transited from uniform pyrolysis along the whole section to the interface centralized pyrolysis along the axial displacement rate distribution. In addition, in an indoor experiment when the pressure is 7.8Mpa the temperature is 350–400 °C, and the injection velocity is 9 ml/s of supercritical carbon dioxide, the effective recovery of shale oil increases from 36% to 97.4% with the increasing temperature and pyrolysis time. However, at the same temperature, the increasing trend of shale oil recovery decreases gradually for an extension of time. The analysis of a combined gas chromatography shows that the shale oil is secondary pyrolysis due to long-term retention in high temperature conditions and thus the increasing trend of oil recovery is gradually eased off

Keyword: Oil shale; Supercritical carbon dioxide (SC-CO₂); Pyrolysis; Oil recovery

1. Introduction

Oil shale is an organic-rich fine-grained sedimentary rock with ty- pical schistosity structure containing kerogen. The oil content of oil shale is 3.5–30%, which also contains the composition of crude oil [1–3]. At present, the main mining methods of oil shale are trans- forming from the earth's surface retorting to underground in-situ pyrolysis [4–7]. The in-situ pyrolysis process of oil shale is based on hydraulic fracturing through injecting high-temperature and high- pressure fluid to dredge the fracture formed by hydraulic fracturing

with simultaneous and continuous input heat to oil shale formation through convective heat transfer. When the temperature reaches the pyrolysis temperature of kerogen, kerogen can be pyrolyzed to produce oil and gas. Driven by high-pressure fluid, the mixture of oil and gas at high-temperature and high-pressure fluid then enters the ground condensation and separation device. The condensation separation device can separate oil, gas and water.

In recent years, new pyrolysis methods have been proposed for oil shale. Zhao et al. simulated high temperature steam pyrolysis of Fushun oil shale under 0.1–2.8 MPa. The results show that oil and gas can be

Table 1

Analysis of oil shale Huadian.

Attribute	Proximate analysis /wt.%				Fisher analysis /wt.%				Elemental analysis /wt.%			
Region	Moisture	Ash	Volatiles	Fixed carbon	oil	Water	Residue	Gas	H	C	N	S
S1	6.75	56.71	25.79	10.75	19.16	6.85	67.04	6.95	4.27	24.96	0.34	1.09
S2	6.68	56.07	26.99	10.26	19.34	6.96	66.83	6.87	4.52	25.86	0.34	1.12

produced continuously only when the temperature is higher than 366–486 °C [8]. Wang et al. used subcritical water as heat carrier to extract shale oil from Huadian oil shale under 16–25 MPa. The results show that when the water/oil shale mass ratio is 3, the maximum ex- tract yield can be reached at 365 °C for 30 h [9]. Sun et al. simulated the topo-chemical heat pyrolysis oil shale under atmospheric pressure. The results show that topo-chemical heat can increase the original temperature of oil shale to 250–300 °C to realize the pyrolysis of oil shale [10,11]. Zhu et al. put forward the technology of microwave heating in- situ pyrolysis of oil shale combined with hydraulic fracturing. Under atmospheric pressure at the power 1000 W, it takes only 10 min to heat oil shale to 750 °C, which can meet the demand of oil shale pyrolysis [12,13]. Sun et al. carried-out pyrolysis experiments of Fuyu oil shale using high voltage breakdown industrial frequency current pyrolysis process. The results show that when the voltage is 1000 V, the break- down current in oil shale is 22A. After 6 min of heating, the heating channel temperature of oil shale reaches 643 °C, which can meet the needs of oil shale pyrolysis [14]. There is no doubt that pressure is an important parameter affecting oil shale pyrolysis, especially in the process of in-situ pyrolysis of oil shale, the influence of reservoir pressure on oil shale pyrolysis cannot be ignored. Although the above described methods can effectively pyrolyze oil shale, the pressure used in the experiment is quite different from the actual formation pressure, simulation, therefore, cannot adequately mimic the actual working conditions of in-situ pyrolysis and it cannot provide reference data for effective in-situ pyrolysis.

The burial depth of Huadian oil shale in the fourth layer is 400–600 m, and the overlying formation pressure is about 9.4 MPa. Therefore, the pressure of high-temperature and high-pressure fluid used in in-situ pyrolysis should be slightly less than 9.4 MPa, otherwise, the pressure is too low to effectively dredge the cracks. Excessive pressure leads to high velocity of fluid flowing through oil shale formation and results in serious energy loss [15]. Supercritical carbon dioxide (SC-CO₂) has the advantages of strong solubility, good diffusion ability and simple formation conditions. It

can be formed when the pressure exceeds 7.6 MPa and the temperature exceeds 35.5 °C. It is suitable for extracting organic matter in porous media as a heat-carrying fluid. When the pressure is 8.0 MPa, the formation fracture can be dredged and the flow rate is suitable. For further details, refer to Zhao et al. 2019 [15]. Although SC-CO₂ is widely used in the gas injection process of oil, natural gas and coalbed methane, little research has been done on the extraction of organic matter from oil shale [16,17].

The oil content of oil shale is low. In the process of underground in situ pyrolysis, the choice of heat-carrying fluid directly affects the oil and gas recovery efficiency [18,19]. This paper presents both experiment and numerical simulation of extraction mechanism of organic matter from oil shale by SC-CO2. Numerical simulation is used to investigate the phenomenon that is difficult to observe directly in the experiment. Firstly, the distribution of SC-CO2 in oil shale during 10–80 h at the injection pressure of 7.8 mpa, injection flow of 2.5–9 ml/s and injection temperature of 400 °C is simulated and analyzed with the COMSOL Multiphysics 5.3a finite element analysis software. The expansion rate of the front represents the flow field distribution of the oil shale pyrolysis front, while the axial velocity represents the displacement rate of shale oil and gas by SC-CO2. The pyrolysis behavior of Huadian oil shale in SC-CO2 is also studied. In order to be consistent with the numerical simulation, the injection pressure, flow rate and temperature of SC-CO₂ are set to be 7.8Mpa, 9 ml/s and 350–400 °C, respectively, and the effective recovery rate of shale oil under the pyrolysis time of 10–80 h is explored. During the experiment, oil and gas products were collected and analyzed using gas chromatography.

2. Material and methods

2.1. Materials

2.1.1. Industrial analysis and elemental analysis

The oil shale of the fourth layer in Gonglangtou mining area of Huadian was used in the test, with a buried depth 400–600 m in a reddish-brown color. The results of proximate and elemental analysis are shown in Table 1.

2.1.2. Thermal conductivity and specific heat capacity analysis

The thermal conductivity of oil shale is different in the parallel di- rection and in the normal direction to bedding, and the thermal de- composition also affects the displacement effect. According to the results of thermogravimetric experiment, seven groups of Huadian oil shale samples were prepared, which are in parallel and normal directions to bedding. The thermal conductivity of Huadian oil shale at different temperatures was measured by Shortherm Qualification Test Model (Zhaohe Electric Industrial Co., Ltd., Japan). The specific heat capacity was measured by BRR specific heat capacity tester (Xiangtan Instruments and Instruments Co., Ltd., China). In addition, the porosity and permeability of oil shale pyrolysis residue at 25–550 °C were measured by mercury intrusion method and nitrogen adsorption method. The results are shown in Table 2.

Table 2
Thermophysical properties of Huadian oil shale residues.

Nature temperature/°C	Thermal conductivity (W/m·°C)		Specific heat capacity (J/kg·°C)	Porosity %	Permeability μm²
	Parallel bedding	Vertical bedding			
25	0.6155	0.5095	2206.0	2.78	$0.12*10^{-5}$
150	0.6951	0.5506	2004.0	4.19	$0.21*10^{-5}$
250	0.4068	0.3282	1733.0	6.23	$0.32*10^{-5}$
350	0.3637	0.3369	1470.7	7.54	$0.37*10^{-5}$
450	0.3568	0.3320	1187.0	8.67	$0.49*10^{-5}$
500	0.2324	0.2177	1033.0	10.03	$0.54*10^{-5}$
550	0.2088	0.1797	764.0	10.86	$0.61*10^{-5}$

2.2. Methods

2.2.1. Numerical simulation method

A three-dimensional model of the combination state of core holder and core in SC-CO$_2$ displacement system is constructed as shown in Fig. 1. In the process of displacement, there is a small gap between the core holder and the core. Therefore, the boundary layer is set as a low permeable and slip free boundary rather than a simple impermeable layer. Oil shale is idealized as a cylinder with a diameter of 20 mm and a length of 30 mm. The top and bottom represent injection and output

Table 3
Parameter calculation for SC-CO$_2$.

Parameter name	unit	Symbol	value
Constant pressure ratio heat capacity	kJ/(kg·K)	Cp	1.147
specific heat at constant volume	kJ/(kg·K)	Cv	0.545
Density	g/cm³	ρ	0.463
Gas viscosity	Pa·s	μ	4.04×10^{-5}
Thermal conductivity	W/(m·K)	λ	46.3
Input temperature	K	T	623.15–673.15
Gas constant	J/(mol·K)	R	8.3144
flow rate	ml/s	Q	2.5–9
Average thermal expansion coefficient	1/K	β	0.00371
Compression coefficient	–	z	0.315

ports of SC-CO2. COMSOL Multiphysics 5.3a was used to simulate the pyrolysis displacement process. Domain mesh and the positions of the monitored curves are shown in Fig. 1.

The specific input parameters of SC-CO2 are shown in Table 3. The permeability of cylindrical porous media is usually calculated by Carman-Kozeny empirical formula [22].

$$k = \frac{\varepsilon^3 D^2}{144(1-\varepsilon)^2} \tag{1}$$

where ε-Porosity; D- diameter [mm].

There is a linear relationship between the axial seepage velocity and the pressure gradient along the core.

$$-\frac{dP}{dx} = \mu \frac{u}{k} \tag{2}$$

where μ – fluid viscosity, [Pa·s]; u – inlet velocity [m/s]; k – permeability coefficient. A large number of studies have shown that the gas permeability measured in low permeability and dense porous media is larger than that of liquid, especially under low pressure, gas molecules do not have close contact with the solid wall. The molecules on the interface are in motion and the velocity is not zero. Therefore, the velocity of gas is larger than that calculated by the Darcy law. If the flow velocity is low and the fluid motion is laminar, the axial seepage velocity of the core satisfies the Eq. (3) [23].

$$u = -\frac{k}{\mu}\Delta P \tag{3}$$

The theoretical solution of pressure distribution in the seepage system satisfies the Eq. (4).

$$P(x) = -b + \sqrt{(P_1^2 - P_0^2 - 2b(P_1 - P_0))\frac{x}{L} + (P_0 + b)^2} \tag{4}$$

where x – core axial distance [mm]; L – core length, 30 mm; b-Klingenberg coefficient;
P0- inlet pressure [MPa]; P1- the pressure at x = L [MPa].
According to the Darcy percolation model of Brinkman-Forchheimer expansion [24,25], when the heat carrying SC-CO2 passes through the pores and the fractures of boundary layer, its mass, momentum and energy are conserved in the heat conduction process of oil shale, that is

$$\nabla \cdot u = 0 \tag{5}$$

$$\frac{\partial u}{\partial t} + u \cdot \nabla\left(\frac{u}{\varepsilon}\right) = -\frac{\nabla \varepsilon P}{\rho} + \mu \nabla^2 u + F \tag{6}$$

$$\sigma\frac{\partial T}{\partial t} + u \cdot \nabla t = \nabla(a\nabla t) \tag{7}$$

$$\sigma = \frac{C}{C_p} \tag{8}$$

where u- flow rate [ml/s]; P- System pressure [MPa]; T- System temperature [K]; ε- Porosity of oil shale; C- Specific heat capacity of oil shale[J/kg·K]; a- Thermal conductivity of oil shale [W/m·K].
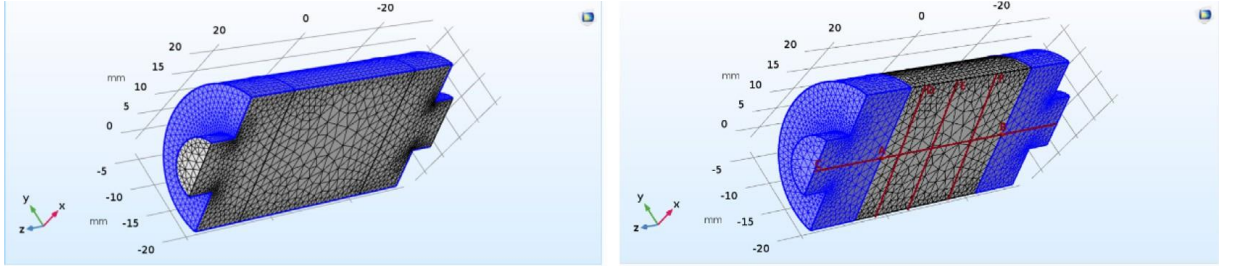F is the resistance of porous media matrix to SC-CO2,

Fig. 1. Pyrolysis and displacement model of Huadian oil shale (a) boundary layer setting (b) monitoring point and monitoring curve setting.

$$F = -\frac{\varepsilon\mu u}{K} - \frac{\varepsilon F_{\varepsilon}}{\sqrt{K}} |u| \, u + \varepsilon G \qquad (9)$$

$$F_{\varepsilon} = 1.75\sqrt{150\varepsilon^3} \qquad (10)$$

$$G = -g\beta(T - T_0) \qquad (11)$$

$$K = \frac{\varepsilon^3 d_p{}^2}{150(1-\varepsilon)^2} \qquad (12)$$

2.2.2. Experimental methods

The working principle and experimental setup of a stainless-steel autoclave as a reactor for oil shale pyrolysis and SC-CO_2 displacement of oil and gas products are illustrated in Fig. 2. Before the start of the experiment, the prepared oil shale sample was put into the core gripper. Open the valve of the high-pressure CO_2 cylinder and inject CO_2 with constant flow rate and constant pressure respectively, at the same time, the air in the reactor is discharged. When CO_2 flows through the gas heater, the temperature rises to 350–400 °C. By setting the heating rate, the termination temperature and the holding time in the temperature control system, the reactor can keep constant temperature in the pre- scribed time. The temperature of the reactor can be kept constant by adjusting the flow rate of CO_2. Paperless recorder is used to record the changes of pressure, velocity and temperature in real time and transmit the data to computer.

According to the gas state equation, the pressure of CO2 in the High Temperature and High-Pressure Heater (HT-HP Heater) at room temperature is set. When the heater is started, the temperature of CO2 in the HT-HP Heater rises and the pressure rises. When the temperature in the reactor reaches the set temperature, the carbon dioxide also reaches the supercritical state. SC-CO2 conducts heat

continuously to oil shale, which makes the temperature of oil shale rise, leading to the pyrolysis of kerogen in oil shale, and the phase-solid state of kerogen changes to gas-phase state. As a result, the pressure in the space where kerogen storage will rise sharply, resulting in a pressure difference between the space of kerogen storage and the pore passage. The pressure difference greater than the fracture pressure in the space of kerogen storage, and oil and gas products will be released into the pore passage. Oil and gas products in pore channels are subjected to unbalanced pressure, and the pressure at the injection face of carbon dioxide is higher than that at the output face, so a pressure difference is formed in the oil shale. Under the joint displacement of pressure difference and carbon dioxide, oil and gas products enter the oil and gas separation device through the output face. The gas is collected into the sampling bag, and the liquid is driven by the piston by a hand pump to continue to be sent to the liquid collection bottle, and weighed by a balance. The composition and content of oil and gas were measured by Gas Chromatography-Mass Spectrometry (GC–MS).

3. Results and discussion

3.1. Numerical simulation

3.1.1. The axial flow velocity

Axial flow rate responds to the displacement efficiency of oil shale pyrolysis process. With the increase of oil shale pyrolysis degree and porosity, the axial flow velocity increase, too. Because the pyrolysis products of oil shale at high temperature exist in gas phase, the higher the axial flow rate, the better the displacement of gas phase products. As can be seen from Fig. 3, time plays an important role in the pyrolysis of oil shale. At different injection velocities, the pyrolysis degree of oil shale increases with time, resulting in porosity increase, which is also conducive to the diffusion of SC-CO_2, so the axial flow velocity in- creases gradually. In addition, injection velocity also plays an important role. To a certain extent, injection velocity is also a measure of injection heat. The

higher injection velocity, the more heat injected per unit time. Therefore, the degree of oil shale pyrolysis increases with the increase of injection velocity in the same time.

In addition, the pyrolysis degree of oil shale decreases from the injection interface to the outflow interface at the same injection velo- city of heat-carrying SC-CO_2. This is because temperature plays an important role in the pyrolysis of oil shale. As shown in Fig. 4 below, for the same oil shale sample, when the flow velocity of heat-carrying SC- CO_2 injection is constant, the minimum principal stress of oil shale will be broken through in unit length, forming a stable path, gradually pe- netrating the whole oil shale. Although the seepage process of heat-carrying SC-CO_2 will lead to the increase of porosity near the seepage path, which is conducive to the diffusion of heat-carrying SC-CO_2. However, when the flow rate is small, the heat loss along the flow path is large, so the degree and quantity of oil shale pyrolysis near the seepage path are limited. With the increase of injection velocity, the heat carrying capacity of SC-CO_2 increases, which leads to the increase of pyrolysis degree and porosity of oil shale near seepage channel. Therefore, the amount of oil shale pyrolysis is more. It also proves that SC-CO_2 has the ability to extract organic matter, and kerogen can be extracted from oil shale even under the condition of temperature lower than that of oil shale pyrolysis. However, when the temperature cannot reach the pyrolysis temperature of oil shale, the extraction efficiency of organic matter and the porosity is low, resulting in a lower axial rate than when the temperature reaches it [20,21].
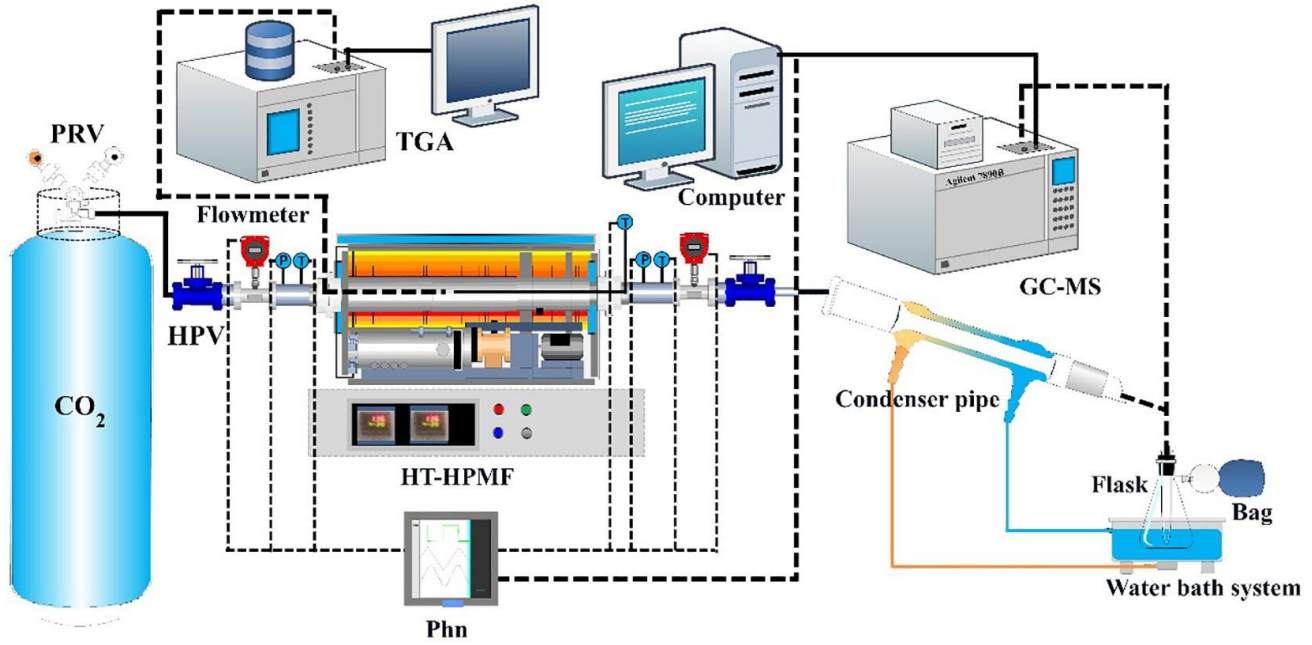

Fig. 2. Experimental schematic diagram of oil shale pyrolysis displacement system.

3.1.2. Entrance effect

To some extent, displacement pressure can reflect the flow rule of fluid and the change of seepage channel in displacement process, whichcan help researchers better master the regulation rule of displacement parameters. In order to reflect the displacement process of shale oil by heat carrying SC-CO2, the whole injection experiment process of heat carrying SC-CO2 is simulated by the method of thermal fluid solid coupling analysis combined with Brinkman equation and Darcy's law. According to the relationship between porosity and temperature, as shown in Table 2, before numerical simulation, set the curve of oil shaleporosity varies with temperature and initial temperature, 25 °C. It is noteworthy that after injection of heat-carrying SC-CO2, there is an obvious "entrance effect" at the interface between oil shale and heat- carrying SC-CO2. The "entrance effect" is the sign of oil shale pyrolysis [20,21]. It is due to the increase of porosity caused by oil shale pyrolysis, which results in the decrease of diffusion pressure from gas phase medium to solid phase skeleton. The pressure gradient of SC-CO2 in oil shale decreases gradually before the oil shale is completely pyrolyzed, which obeys Brinkman's extended Darcy's law. This is because the seepage channel has not been formed, and only a small part of weakfluid reaches the outlet interface, so the pressure is small. However, with the increase of diffusion distance, the percolation channel of supercritical carbon dioxide in oil shale is gradually formed. The pore channels of oil shale are complex and the resistance along the process increases, so the pressure shows an increasing trend.

However, after pyrolysis of oil shale, pore channels are gradually opened, so the pressure distribution is basically stable and increases with the increase of diffusion distance. In addition, the larger the injection flow rate, the more obvious the trend of "entrance effect" in the same pyrolysis time, and the pressure of oil shale diffusion will be lower. As shown in Fig. 5, after 10 h of pyrolysis of oil shale at 400 °C, the inlet pressure of SC-CO2 at the two-phase interface is 7.62 MPa at the injection rate of 2.5 ml/s. When the injection flow rate is 9.0 ml/s, the inlet pressure of SC-CO2 at the interface of two phases is 3.77 MPa. What's more, at the same injection flow rate, the diffusion pressure willgradually decrease with time. This is because with the prolongation of pyrolysis time, the "entrance effect" of oil shale increases and more heat-carrying SC-CO2 diffuses into oil shale. This will promote the pyrolysis of internal oil shale, increase porosity and promote the ex-pansion of seepage channels.
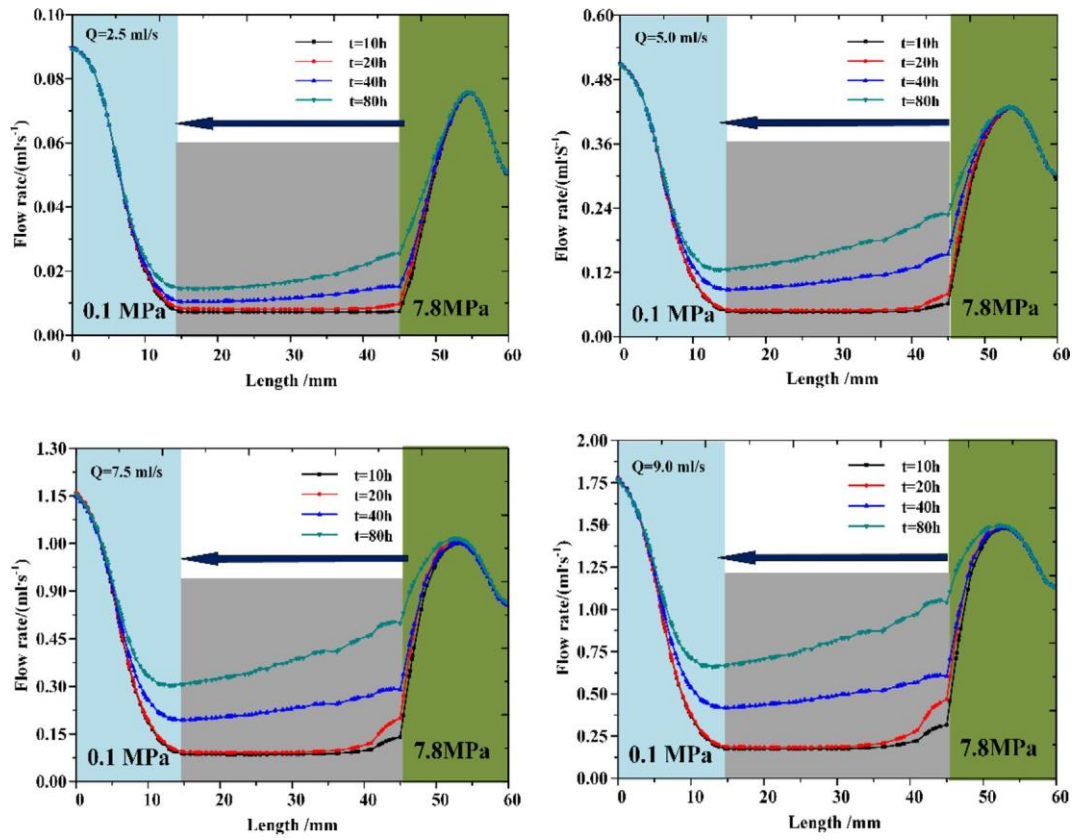
Fig. 3. Axial flow velocity of SC-CO_2 varies with time and injection velocity (a)Q = 2.5 ml/s; (b) Q = 5.0 ml/s; (c) Q = 7.5 ml/s; (d) Q = 9.0 ml/s.

3.1.3. Outlet interface flow velocity

The displacement front velocity is a characterization of the pyrolysis rate of oil shale. This velocity can be measured by the outlet interface, as shown in Fig. 6 below. The velocity of displacement front is significantly affected by pyrolysis time and SC-CO_2 injection flow rate.

When oil shale pyrolysis is not completed, especially when the seepage channel is not fully dredged, the boundary velocity of displacement front is higher than the central velocity due to the low porosity of the oil shale, and the seepage coefficient of core holder and oil shale boundary is larger than that of the internal pore of oil shale.

When the pyrolysis time exceeds 40 h, the changes of flow rate at the outlet interface occure. The velocity in the center of oil shale increases gradually, until it is higher than that of the boundary velocity.
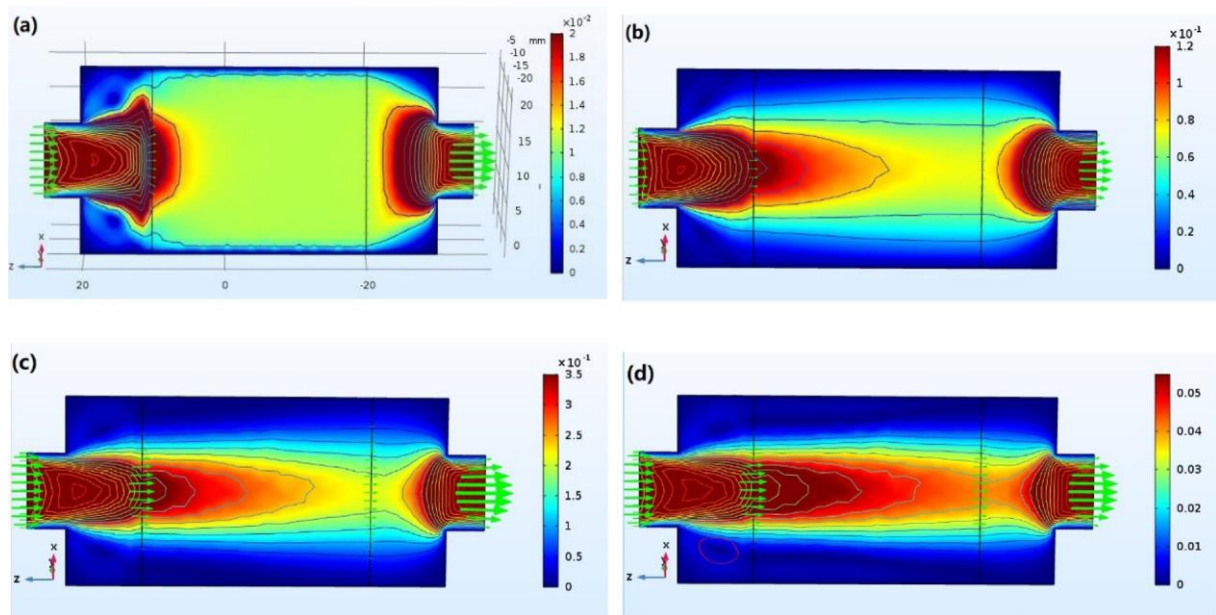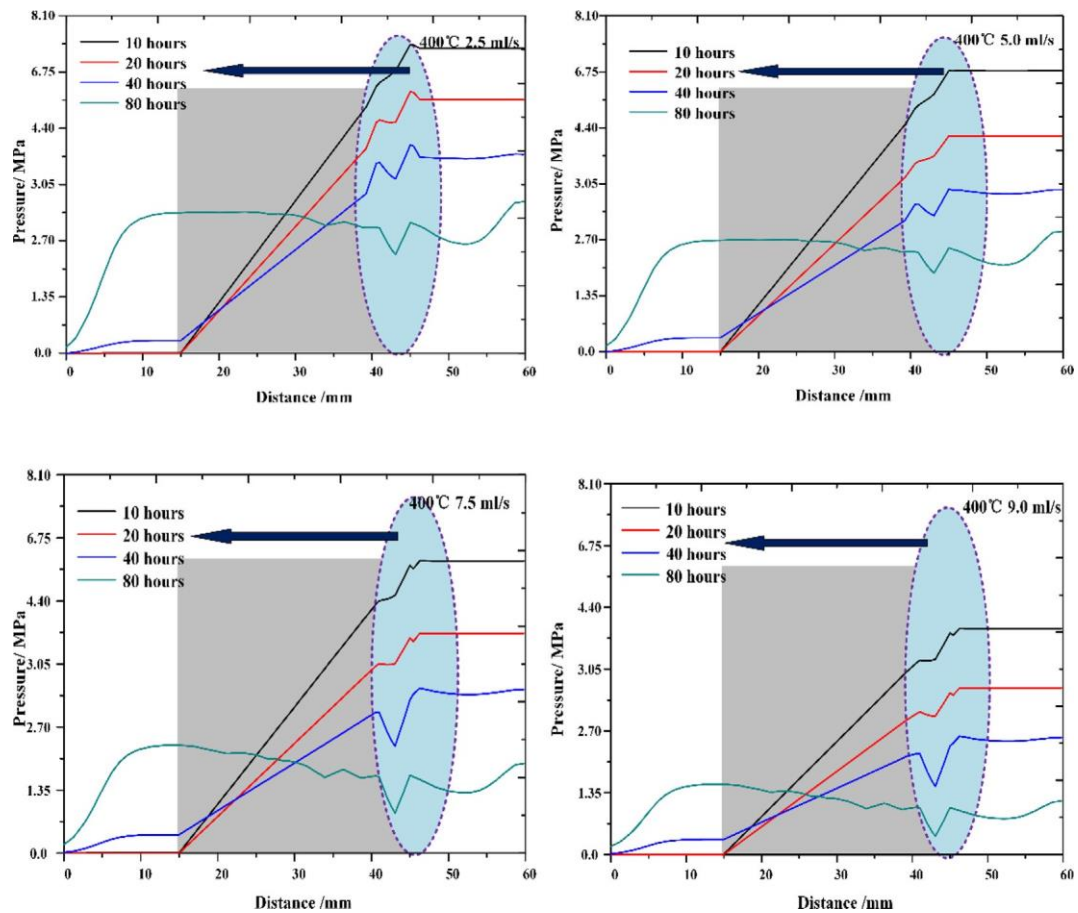
Fig. 4. The diffusion path of heat carrying SC-CO$_2$.

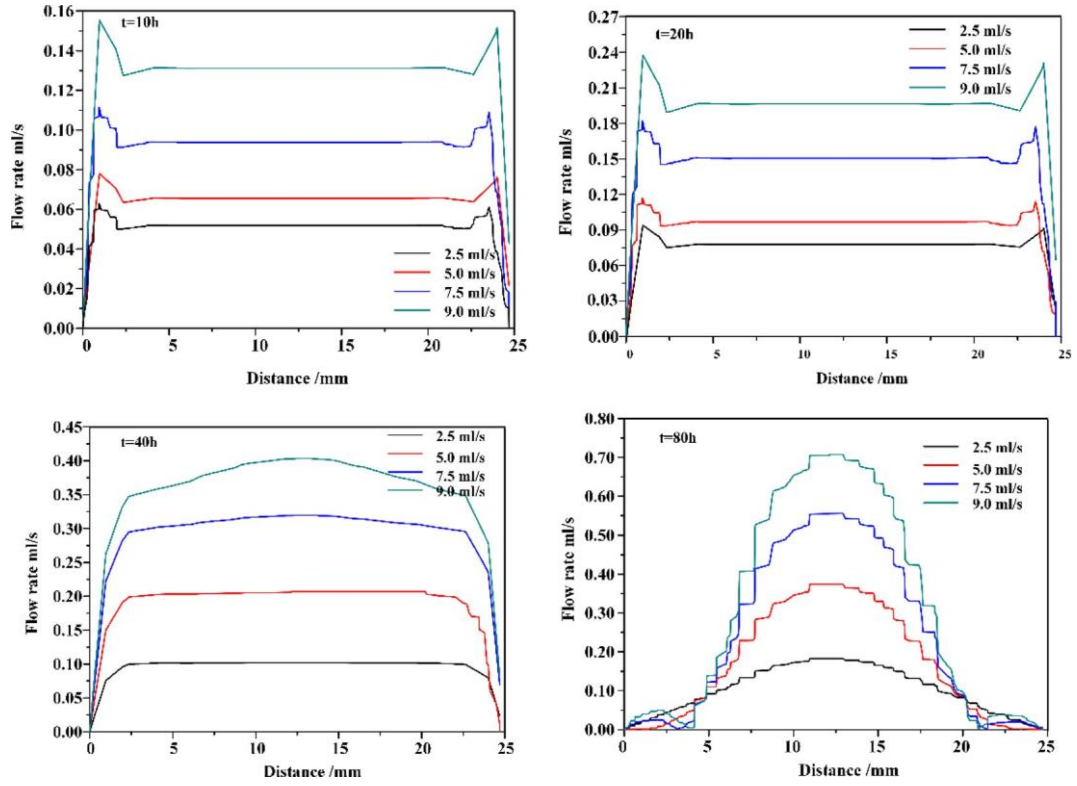Fig. 5. Pressure distribution and "entrance effect" of oil shale pyrolysis.

Fig. 6. Velocity distribution of displacement front varies with time and injection flow rate (a) t = 10 h (b) t = 20 h; (c) t = 40 h; (d) t = 80 h.
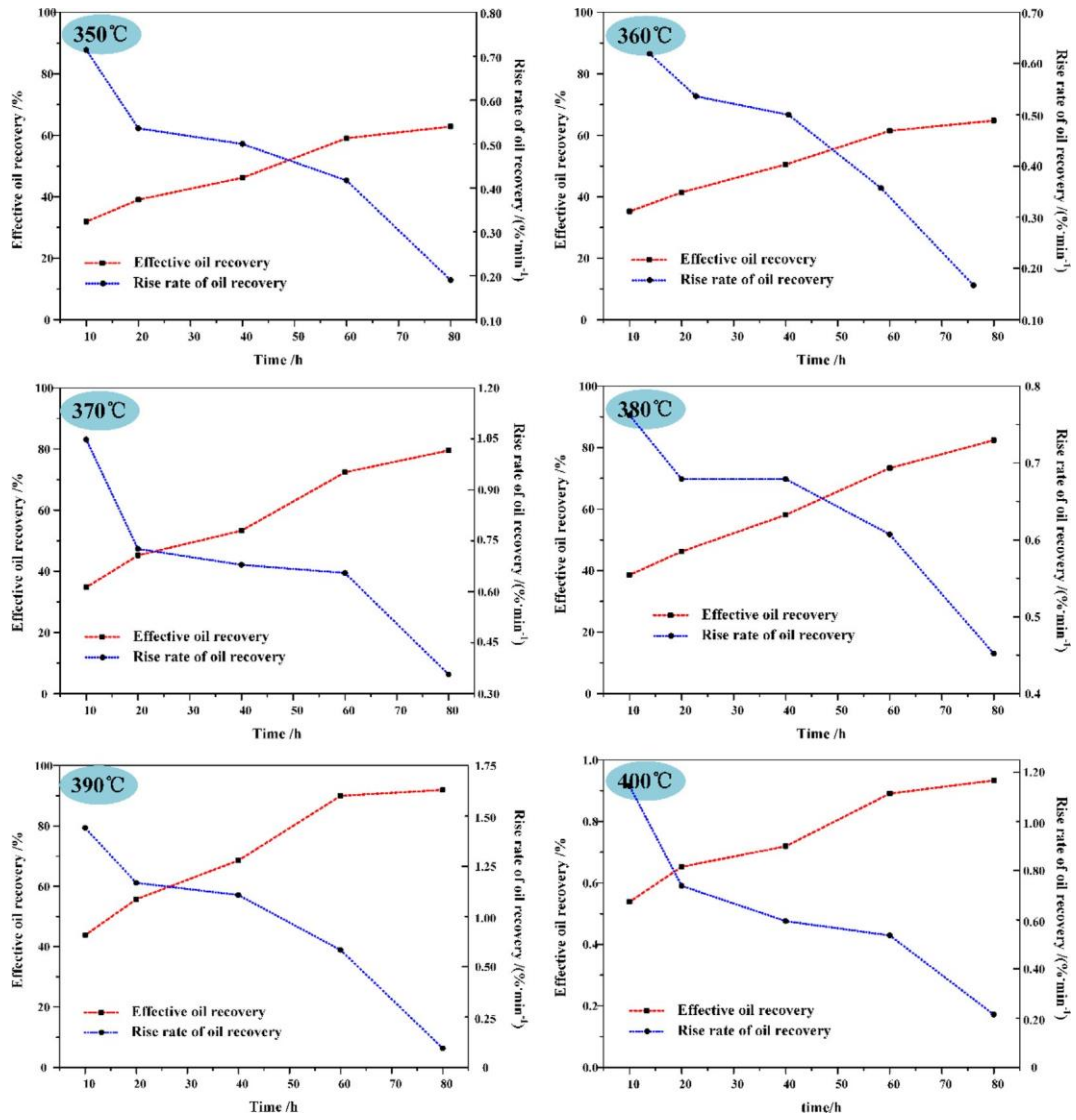
Fig. 7. Oil recovery of oil shale by SC-CO$_2$ extraction under400 °C.

This is due to the time prolongation in heat-carrying SC-CO2 which flows through the oil shale to form a stable seepage channel. With the increase of injection flow rate and continuous pyrolysis process, the porosity and the thermal conductivity of oil shale increase, which weakens the marginal seepage velocity of oil shale and the dominant heat transfer mechanism transits from conduction to convection. As the pyrolysis process of oil shale continues to advance, the porosity continues to increase. After 80 h, the displacement front rate reaches peaks. And with the increase of injection rate, the peak value increases, enhancing the convective heat transfer effect and resulting in more efficient heat transfer for the rapid flow of heat-carrying SC-CO2 in oil shale and in the pyrolysis process.

3.2. Rate of oil recovery

During each experiment, the quality of oil shale particles samples is about 100 g. The flow rate of SC-CO2 into the reactor is 9.0 ml/s.

According to the model of effective oil recovery in the process of oil exploitation, the effective recovery of shale oil is calculated by the following equations:

$$\eta = \frac{E_1}{E_0} \times 100\% \tag{13}$$
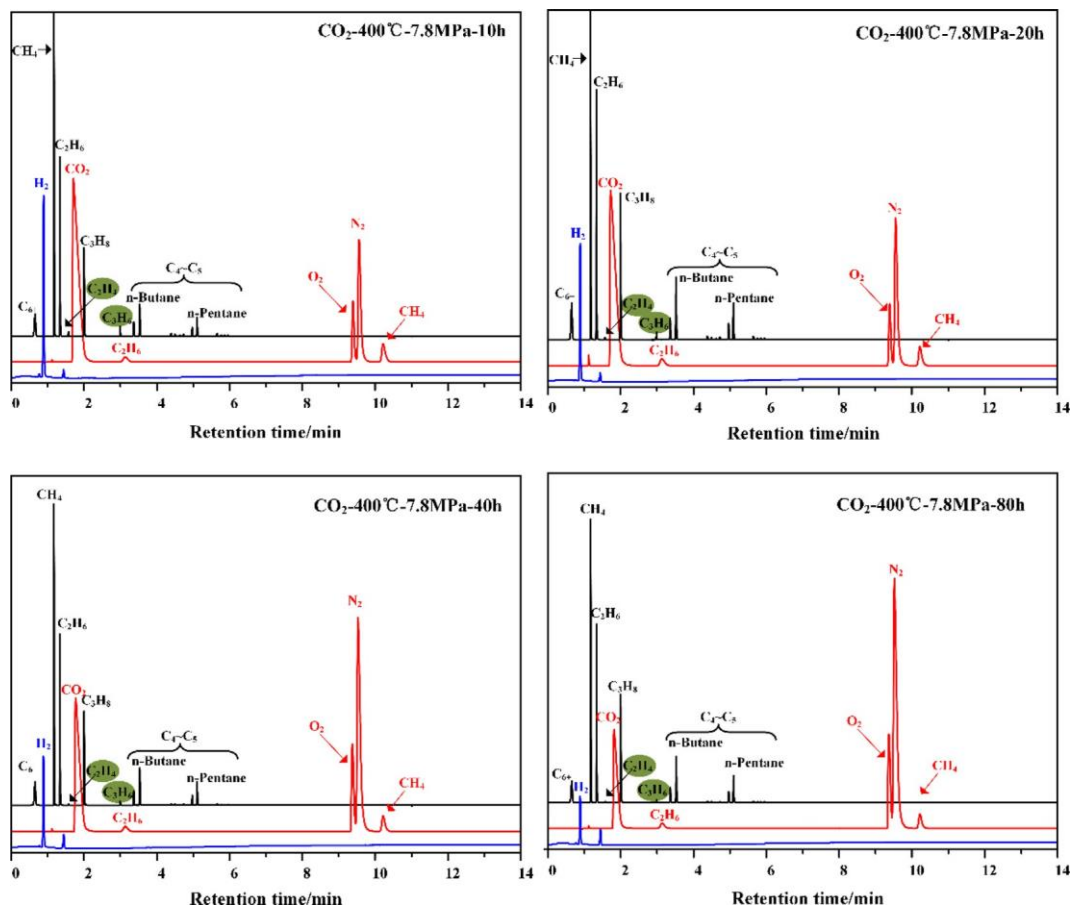
$$E_1 = \frac{m_1}{m_0} \times 100\% \tag{14}$$

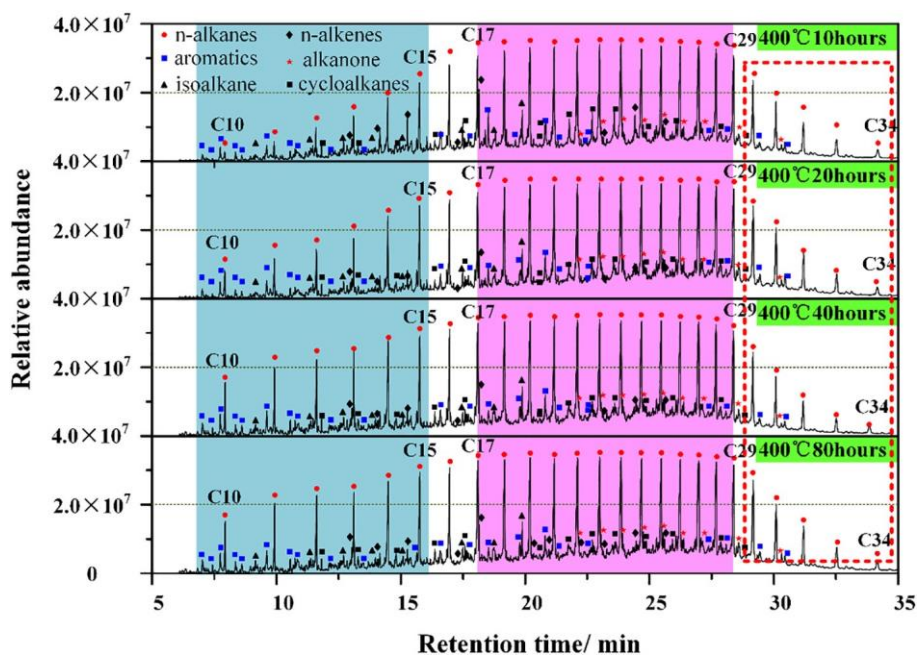Fig. 8. Chromatographic analysis of pyrolysis gas by SC-CO_2 extraction under 400 °C.

Fig. 9. Analysis shale oil by gas chromatography and mass spectrometry under 10–80 h.
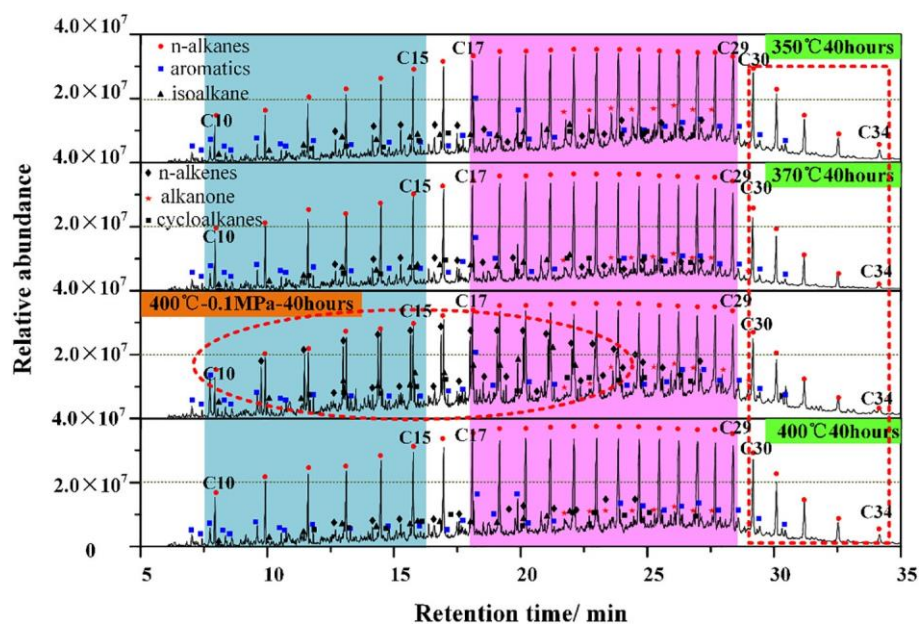
Fig. 10. Analysis of shale oil by gas chromatography and mass spectrometry under different conditions.

where E0- oil content, 19.2%; m1- quality of shale oil collected in the experiment, g; m0- quality of oil shale in the experiment [g]. At this time, the temperature of the reactor is 350–400 °C, and the holding time is 10–80 h. After the test, the oil, gas and residue were collected and analyzed. As shown in Fig. 7, the curve of oil recovery is obtained when the temperature of the reactor is 350–400 °C. The oil content of Huadian oil shale is only about 19.2%. The curve shows that the oil recovery increases with the SC-CO2 induced time prolongation. Furthermore, the higher the pyrolysis temperature is, the more obvious the trend is. However, when the induction time of each group increases to 60 h, the oil recovery increases are almost unnoticeable. This is mainly because some of the accumulation of oil shale particles affect the heat and mass transfer process of SC-CO2 to oil shale, and also affect the displacement process of SC-CO2 in the process of oil and gas precipitation. Therefore, the time of induction to pyrolysis oil shale is 60 h, which basically achieves the best oil recovery. In addition, the treatment temperature has also a great influence on the oil recovery. The oil recovery of 10 h induced by SC-CO2 is only about 36% at the temperature 350 °C. But the oil recovery of 10 h reaches about 56.2% at the temperature 400 °C, For 80-hour pyrolysis time, the oil recovery is 63.7% at the temperature 350 °C whilst at the temperature 400 °C, the oil recovery reaches 97.4%.

3.3. Gas chromatography and mass spectrometry

Under different temperatures and time conditions, the shale oil and gas obtained by extracting organic matter from oil shale by heat-carrying SC-CO2 were collected for gas chromatography and mass spectrometry analysis. In addition, contrast analysis of supercritical state is also performed using a series of extraction experiments of CO2 under atmospheric pressure.

As shown in Fig. 8, methane, ethane and propane present the main gas products in the pyrolysis of oil shale with SC-CO2. In addition, the components of the gas include hydrogen, isomers of butane and pentane, ethylene and propylene. At the temperature 400 °C, the contents of methane, ethane and propane increased with the increase of pyrolysis time, but decreased when the pyrolysis time exceeded 40 h. The main reason for this phenomenon is due to the prolongation of the retention time of oil and gas products in oil shale. The extension of retention time will lead to the aggravation of secondary cracking of oil and gas products, and the generation of a large number of free methyl and hydrogen radicals, which easily react with unsaturated hydro- carbons, leading to the reduced content of ethylene and propylene. In addition, free methyl and hydrogen radicals will react with macro- molecular unsaturated hydrocarbons to form more shale oil, as observable from the later stage of oil yield curve at the temperature 400 °C.

The results of gas chromatography and mass spectrometry (Figs. 9 and 10) show that the components of shale oil extracted by heat carrying SC-CO2 at different temperatures are similar, including mainly n- alkanes, isoalkanes, cycloalkanes, alkenes, aromatics and alkanones with a small amount of alkanoic acid. Compared to the methods of topochemical reaction method [11] and subcritical water extraction [26], the obtained components of aromatic compounds in shale oil by pyrolysis are higher using heat-carrying SC-CO2, indicating that carbon dioxide is involved in the reaction of oil and gas products in porous media at high

temperatures. The main components of alkanes in shale oil are C17–C29. The operating time and temperature have a great in- fluence on the composition of shale oil. The aggravation of secondary cracking happens by either extending the pyrolysis time or increasing the temperature of heat-carring SC-CO$_2$.. The secondary cracking, to some extent, breaks the chemical bond of macromolecular substances (e.g. C30–C34) and produces more small molecular substances (e.g. C10–C15). In addition, according to the heteropeak display at the bottom of chromatograms in Figs. 9 and 10 and the extraction results under different times, temperatures and pressures, increasing tem- perature and pyrolysis pressure, and extending pyrolysis time inhibit the generation of aromatic compounds. Altogether, it can be concluded that the formation of alkenes is inhibited by high pressure.

4. Conclusion

Supercritical carbon dioxide can effectively extract organic matter from oil shale, however, retention time, pyrolysis temperature and environmental pressure all affect the pyrolysis process of oil shale. The simulations show that increasing injection flow and residence time can make the displacement interface more centralized, and increase the displacement rates. Under SC-CO$_2$ condition, the composition of aromatic hydrocarbon in shale oil increases. Prolonging the pyrolysis time and increasing the temperature of SC-CO$_2$ can lead to the aggravation of secondary cracking and the formation of short chain alkanes. In addition, pressure also affects the generation of alkenes. Increasing pressure causes the decrease of alkenes content in shale oil. The extension of pyrolysis temperature and time reduces the content of aromatic com- pounds in shale oil.

CRediT authorship contribution statement

Zhao Shuai: Complete the process of experiment and article writing. Lü Xiaoshu: Complete article review and language editing. Li Qiang: Complete the reactor design and participate in the experimental process. Sun Youhong: Provide ideas, guide the experimental process, and help to communicate with foreign authors.

Declaration of Competing Interest

The authors declare that they have no known competing financial interests or personal relationships that could have appeared to influence the work reported in this paper.

References

[1] K. Rajeshwar, R. Nottenburg, J. Dubow, Thermophysical properties of oil shales, J. Mater. Sci. 14 (1979) 2025–2052.

[2] M.F. Martins, S. Salvador, J.F. Thovert, et al., Co-current combustion of oil shale – Part 1: characterization of the solid and gaseous products, Fuel 89 (2010) 144–151.

[3] J.G. Na, C.H. Im, S.H. Chung, et al., Effect of oil shale retorting temperature on shale oil yield and properties, Fuel 95 (2012) 131–135.

[4] J. Jaber, S.D. Probert, Environmental-impact assessment for the proposed oil-shale integrated tri-generation plant, Appl. Energy 62 (1999) 169–209.

[5] X.X. Han, X.M. Jiang, Z.G. Cui, Studies of the effect of retorting factors on the yield of shale oil for a new comprehensive utilization technology of oil shale, Appl. Energy 86 (2009) 2381–2385.

[6] A.R. Brandt, Converting oil shale to liquid fuels: Energy inputs and greenhouse gas emissions of the Shell in situ conversion process, Environ. Sci. Technol. 42 (2008) 7489–7495.

[7] D.X. Liu, H.Y. Wang, D.W. Zheng, et al., World progress of oil shale in-situ ex-ploitation methods, Nat. Gas. Ind. 29 (2009) 128–132.

[8] L. Zhao, D. Yang, Z.Q. Kang, et al., Gas generation law of oil shale heated by su-perheated steam, J. Taiyuan Univ. Technol. 46 (3) (2015) 323–326.

[9] Zhijun Wang, Sunhua Deng, Gu. Qiang, et al., Subcritical water extraction of hua-dian oil shale under isothermal condition and pyrolysate analysis, Energy Fuels 28 (2014) 2305–2313.

[10] You-Hong Sun, Feng-Tian Bai, Lu. Xiao-Shu, et al., A novel energy-efficient pyr-olysis process: self-pyrolysis of oil shale triggered by topochemical heat in a hor-izontal fixed bed, Sci. Rep. 5 (2015) 1–8.

[11] Youhong Sun, Fengtian Bai, Baochang Liu, et al., Characterization of the oil shale products derived via topochemical reaction method, Fuel 115 (2014) 338–346.

[12] Jingyi Zhu, Zhaozhong Yang, Xiaogang Li, et al., Application of microwave heating with iron oxide nanoparticles in the in-situ exploitation of oil shale, Energy Sci. Eng. 6 (2018) 548–562.

[13] Zhaozhong Yang, Jingyi Zhu, Xiaogang Li, et al., Experimental Investigation of the Transformation of Oil Shale with Fracturing Fluids under Microwave Heating in the Presence of Nanoparticles, Energy Fuels 31 (2017) 10348–10357.

[14] Sun Youhong, Zhao Shuai, Li Qiang, et al., Thermoelectric coupling analysis of high-voltage breakdown industrial frequency pyrolysis in Fuyu oil shale, Int. J. Therm. Sci. 130 (2018) 19–27.

[15] Shuai Zhao, Youhong Sun, Haoran Wang, et al., Modeling and field-testing of fracturing fluid back-flow after acid fracturing in unconventional reservoirs, J. Petrol. Sci. Eng. 176 (2019) 494–501.

[16] I. Gaus, M. Azaroual, L.I. Czernichowski, Reactive transport modeling of the impact of CO_2 injection on the clayey cap rock at sleipner (north sea), Chem. Geol. 217 (3–4) (2005) 319–337.

[17] S. Bouquet, A. Gendrin, D. Labregere, et al., CO2CRC Otway Project, Australia: Parameters Influencing Dynamic Modeling of CO_2 Injection into a Depleted Gas Reservoir. Offshore, Europe. (2009).

[18] A.C. Aycaguer, L.O. Miriam, A.M. Winer, Reducing carbon dioxide emissions with enhanced oil recovery projects: a life cycle assessment approach, Energy Fuels 15 (2) (2001) 303–308.

[19] N. Morteza, M. Samane, Y.G. Gu, Effects of viscous and capillary forces on CO_2 enhanced oil recovery under reservoir conditions, Energy Fuels. 21 (6) (2007) 3469–3476.

[20] Y.G. Li, N. Zhang, W.F. Lu, et al., Numerical study on inlet effect of foam flow process in a porous media, J. Eng. Thermophys. 38 (9) (2017) 1960–1964.

[21] Z.S. Chen, M.Z. Xie, H.S. Liu, et al., An investigation into characteristics of turbu-lence within big-cavity porous media, J. Eng. Thermophys. 1 (2013) 189–193.

[22] A. Nakayama, F. Kuwahara, Y. Kawamura, Koyama. Three-dimensional numerical simulation of flow through a microscopic porous structure. Proceedings of the ASME·JSME Thermal Engineering Joint Conference. 1995,3:313-318.

[23] R.U. Zhongliang, J.I.A.N. Kuo, M.A. Guosheng, The gas seepage model in porous medium considering Klinkenberg effect, China Sciencepaper 3 (2018) 310–313.

[24] T. Clemens, K. Wit, T. Clemens, et al., CO_2 enhanced gas recovery studied for an example gas reservoir, Soc. Petrol. Eng. (2002).

[25] A.V. Radaev, N.R. Batrakov, A.A. Muhamadiev, A.N. Sabirzyanov, Effect of ther-mobaric conditions in a uniform bed on the displacement of low-viscosity oil by supercritical carbon

dioxide, Russian J. Phys. Chem. B 3 (8) (2009) 1134–1139.

[26] Youhong Sun, Shijie Kang, Siyuan Wang, et al., Subcritical water extraction of huadian oil shale at 300 degrees C, Energy Fuels 33 (3) (2019) 2106–2114.